

Formation of Supported Bilayers on Silica Substrates

Travers H. Anderson,[†] Younjin Min,[†] Kim L. Weirich,[‡] Hongbo Zeng,[†] Deborah Fygenon,^{‡,§} and Jacob N. Israelachvili^{*,†,‡}[†]Department of Chemical Engineering and [‡]Graduate Program in Biomolecular Science and Engineering and [§]Department of Physics, University of California at Santa Barbara, Santa Barbara, California 93106

Received January 15, 2009. Revised Manuscript Received March 2, 2009

We have investigated the formation of phospholipid bilayers of the neutral (zwitterionic) lipid dimyristoyl-phosphatidylcholine (DMPC) on various glass surfaces from vesicles in various aqueous solutions and temperatures using a number of complementary techniques: the surface forces apparatus (SFA), quartz crystal microbalance (QCM), fluorescence recovery after photobleaching (FRAP), fluorescence microscopy, and streaming potential (SP) measurements. The process involves five stages: vesicle adhesion to the substrate surfaces via electrostatic and van der Waals forces, steric interactions with neighboring vesicles, rupture, spreading via hydrophobic fusion of bilayer edges, and ejection of excess lipid, trapped water, and ions into the solution. The forces between DMPC bilayers and silica were measured in the SFA in phosphate buffered saline (PBS), and the adhesion energy was found to be 0.5–1 mJ/m² depending on the method of bilayer preparation. This value is stronger than the expected adhesion predicted by van der Waals interactions. Theoretical analysis of the bilayer–silica interaction shows that the strong attraction is likely due to an attractive electrostatic interaction between the uncharged bilayer and negatively charged silica owing to the surfaces interacting at “constant potential.” However, the bilayer–silica interaction in distilled water was found to be repulsive at all distances, which is attributed to the surfaces interacting at “constant charge.” These results are consistent with QCM measurements that show vesicles readily forming bilayers on silica in high salt but only weakly adhering in low salt conditions. We conclude that the electrostatic interaction is the most important interaction in determining the adhesion between neutral bilayers and charged hydrophilic surfaces. SP and FRAP experiments gave insights into the bilayer formation process as well as information on the surface coverage, lateral diffusion of the lipid molecules, and surface potential of the bilayers during the spreading process.

Introduction

Lipids are biological, amphiphilic molecules that self-assemble into different types of structures (planar, cylindrical, spherical, lamellar, and bicontinuous three-dimensional networks). Planar lipid bilayers are the basic building blocks of biological cell membranes, defining the cell, nucleus, and organelles such as the mitochondria. Closed shell bilayers, also known as vesicles, abound in the cytoplasm and are involved in complex processes such as adhesion, fusion, budding, and cellular transport. The simplicity of bilayer and vesicle structures eludes the complex molecular forces and interactions that determine their size, shape, and stability, and their interactions with other bilayers, vesicles, and surfaces, both biological and nonbiological.

Phospholipid bilayers supported on solid substrates such as glass are of interest for understanding cell–substrate interactions, for developing (bio)chemical sensors, catalytic surfaces, or immobilized protein arrays, and as nanometer-thick insulating layers on conductive surfaces.^{1–7} They are also of general fundamental interest for understanding complex colloidal systems, including nanoparticle dispersions.

Supported phospholipid bilayers are commonly produced either by Langmuir–Blodgett (LB) deposition or by vesicles adsorbing or “self-assembling” from solution. LB deposition is quantitative and controllable but slow and unscalable. Adsorption from solution is neither well-understood nor well-controlled, but it holds promise for fast large-scale preparation of bilayer-coated surfaces. Despite the considerable work on vesicle adsorption during the 20 years since the pioneering work of McConnell and co-workers,^{1,6,8} there is still no clear picture of the forces and various stages that a vesicle goes through as it adheres, fuses, and spreads on a solid surface.^{9–15} Understanding and controlling the transformation of vesicles in solution into a continuous and stable single bilayer on a surface would provide a potentially important tool for functionalizing surfaces, both planar and porous.

In this study, we have employed a number of complementary techniques to measure vesicle adsorption and to characterize the resulting bilayers on various glass surfaces under different solution conditions. A surface forces apparatus (SFA) was used to measure the forces between silica and DMPC bilayers supported on mica. A quartz crystal microbalance (QCM) was used to monitor the dynamics of bilayer adsorption on silica. Fluorescence microscopy (FM) imaging and fluorescence recovery after

*To whom correspondence should be addressed. E-mail: jacob@engineering.ucsb.edu.

(1) Tamm, L. K.; McConnell, H. M. *Biophys. J.* **1985**, *47*(1), 105–113.
(2) Helm, C. A.; Israelachvili, J. N.; McGuiggan, P. M. *Science* **1989**, *246*(4932), 919–922.
(3) Sackmann, E. *Science* **1996**, *271*(5245), 43–48.
(4) Parikh, A. N.; Groves, J. T. *MRS Bull.* **2006**, *31*(7), 507–512.
(5) Cornell, B. A.; Braach-Maksvytis, V. L. B.; King, L. G.; Osman, P. D. J.; Raguse, B.; Wiczorek, L.; Pace, R. J. *Nature (London)* **1997**, *387*(6633), 580–583.
(6) Brian, A. A.; McConnell, H. M. *Proc. Natl. Acad. Sci. U.S.A.* **1984**, *81*(19), 6159–6163.
(7) Bieri, C.; Ernst, O. P.; Heyse, S.; Hofmann, K. P.; Vogel, H. *Nat. Biotechnol.* **1999**, *17*(11), 1105–1108.

(8) McConnell, H. M.; Watts, T. H.; Weis, R. M.; Brian, A. A. *Biochim. Biophys. Acta* **1986**, *864*(1), 95–106.
(9) Heine, D. R.; Rammohan, A. R.; Balakrishnan, J. *Mol. Simul.* **2007**, *33*(4–5), 391–397.
(10) Reviakine, I.; Brisson, A. *Langmuir* **2000**, *16*(4), 1806–1815.
(11) Johnson, J. M.; Ha, T.; Chu, S.; Boxer, S. G. *Biophys. J.* **2002**, *83*(6), 3371–3379.
(12) Schonherr, H.; Johnson, J. M.; Lenz, P.; Frank, C. W.; Boxer, S. G. *Langmuir* **2004**, *20*(26), 11600–11606.
(13) Richter, R. P.; Brisson, A. R. *Biophys. J.* **2005**, *88*(5), 3422–3433.
(14) Reimhult, E.; Hook, F.; Kasemo, B. *Langmuir* **2003**, *19*(5), 1681–1691.
(15) Richter, R. P.; Berat, R.; Brisson, A. R. *Langmuir* **2006**, *22*(8), 3497–3505.

photobleaching (FRAP) experiments were used to observe the surface coverage and the lateral diffusion of the lipid molecules in the bilayers. Streaming potential (SP) measurements were carried out to establish the changing surface potential with time and correlate it with the bilayer adsorption. The combination of these experiments, together with some theoretical modeling of surface interactions involved, provides a fairly comprehensive picture of the vesicle adhesion, fusion, and spreading processes which should be applicable to other surfaces.

Materials and Methods

Vesicle Preparation. 1,2-Dimyristoyl-*sn*-glycero-3-phosphocholine (DMPC), Avanti, was used for the SFA and QCM experiments, and a mixture of DMPC with 1,2-dimyristoyl-*sn*-glycero-3-phosphoethanolamine-*N*-(7-nitro-2-1,3-benzoxadiazol-4-yl) (NBD-PE), Avanti, was used for the fluorescent microscopy experiments. For QCM, fluorescence microscopy, and some SFA experiments, vesicles were prepared by extrusion.¹⁶ Briefly, the lipids were dissolved and mixed in chloroform and then dried by purging with nitrogen gas and stored in a vacuum desiccator. Dried lipids were hydrated in a phosphate buffered saline solution (PBS, Aldrich) and then subjected to 5–10 freeze–thaw cycles consisting of freezing in liquid nitrogen followed by thawing in a warm water bath (~45 °C) until the temperature of the solution had equilibrated with that of the bath. The resulting vesicle solution was then extruded 10 times through polycarbonate membranes of decreasing pore size: first 200 nm, then 100 nm, and finally 50 nm. Care was taken to ensure the extrusion took place above the chain melting temperature of DMPC. Vesicle size was verified by dynamic light scattering (Brookhaven Laser Light Scattering instrument with an Avalanche photodiode detector) and found to have a diameter of ~75 nm. The vesicle dispersion was stable in the buffer solution, which was stored in a refrigerator until use.

Surface Forces Apparatus (SFA) Measurements. Surface forces experiments were carried out in an SFA 2000 as previously described.¹⁷ All water used in preparing the solutions and as a subphase for the LB deposition was purified by a Milli-Q (Elix-10 and Milli-Q Gradient A10) water purification system. Mica surfaces were prepared and mounted on silica discs as previously described.¹⁸ The amorphous silica surfaces for the SFA experiments were prepared by electron-beam deposition on mica as described by Vigil et al.¹⁹ and cleaned in an argon-water plasma to ensure cleanliness and hydrophilicity. DMPC bilayers on the opposing mica surface were deposited by either vesicle fusion or LB deposition. Bilayers deposited by vesicle fusion were done so by allowing the mica surface to incubate in a 1 mg/mL solution of DMPC followed by rinsing in clean buffer. Bilayers deposited by LB deposition were deposited at 28 °C and at a surface pressure of 42 mN/m corresponding to an area per headgroup of 59 Å². The bilayers were allowed to equilibrate in solution saturated with DMPC for a minimum of 1 h to allow relief of any residual stresses in the bilayer and ensure that the headgroup area of each type of bilayer was not a significant variable in the experiments. After deposition of the bilayer, care was taken to transport and mount the surface under water, avoiding any exposure to air. Experiments were carried out at 28 °C, above the chain melting temperature of DMPC. After mounting opposing silica and bilayer surfaces in the SFA, the apparatus was placed in position for experiments

with the light source passing through the surfaces and temperature was allowed to equilibrate for 1 h before each experiment began. Experiments were carried out in PBS and Milli-Q water, both saturated with DMPC at the critical micelle concentration (CMC) by overnight equilibration with excess lipid.

Quartz Crystal Microbalance (QCM) Measurements. A QCM (Q-Sense QCM-D 300) was used to measure the rate of adsorption and rupture of vesicles onto amorphous silica QCM crystals (Q-Sense). Crystals were reused up to 10 times. Before each use, crystals were cleaned in 2% SDS solution, rinsed thoroughly in Milli-Q water and ethanol, and then treated with UV-ozone and finally rinsed again with Milli-Q water.

Fluorescence Microscopy and Fluorescence Recovery after Photobleaching (FRAP). FRAP studies were carried out on bilayers deposited from vesicles containing a small percentage (2–4%) of fluorescently labeled lipid molecules (NBD-PE). Flowcells were constructed by mounting a clean coverglass (borosilicate, Fisherbrand; zinc titanate, Corning; and silica, Technical Glass Products) on two parafilm spacers, forming a thin channel, resting on a clean microscope slide (Gold Seal) and heating to seal. All glass was cleaned by rinsing in water and ethanol, and treating with UV/ozone (UVOCS) for 30 min and stored under vacuum in a glass desiccator (Wheaton, Dry Seal) until use. The flowcell was initially filled with PBS buffer of the same ionic strength as the vesicle solution. Approximately 3 volumes of vesicle solution were then passed through the flowcell. Vesicle solution was then left to incubate in the flowcell for 5 min before rinsing (flushing) with approximately 18 volumes of pure PBS buffer to reduce the background fluorescence signal. Temperature changes at the microscope were attained by placing a brass block, held at 32 or 12 °C by circulating water from a bath, in contact with the microscope slide. Temperature was measured by using a thermocouple sandwiched between the block and the microscope slide.

The sample was imaged in epifluorescence using an Olympus IX-70 microscope with a 40×/0.75 NA objective (Olympus) and a CCD camera (Sensicam-qe, Cooke, Corp.). To probe the continuity and fluidity of the bilayer, a spot approximately 75 μm in diameter was illuminated with light from a Hg-arc lamp for 20 s to irreversibly darken (bleach) the fluorescent lipid molecules in the region. Images were collected at regular intervals under wide-field attenuated illumination to monitor the fluorescence recovery of the darkened spot.

Streaming Potential Measurements. A new miniaturized streaming potential apparatus (SPA) based on a previous model²⁰ was developed to measure surface potentials while simultaneously imaging the surface with a fluorescence microscope (Figure 1). The SPA consists of a channel formed by a pair of flat, parallel solid surfaces, a Teflon “reference” surface and a transparent “glass” surface, with an inlet and an outlet compartment at either end. The channel, 12 mm long × 7 mm wide × 0.08 mm high, was formed by clamping the two surfaces to a spacer providing the 0.08 mm gap between the surfaces. A syringe pump (Standard Infuse/Withdraw Harvard 33 Twin Syringe Pumps, MA) was used to create flow through the channel, and flow rates were carefully calibrated before experiments. Each flow rate was then converted to its corresponding pressure based on the appropriate hydrodynamic equation.²¹ The streaming potential in the cell was measured by using two Ag/AgCl electrodes (Bioanalytical Systems, Inc.), one in each compartment, using an electrometer (Keithley Instruments, Inc. model 6514). To determine the surface potential ζ, a series of

(16) Hope, M. J.; Bally, M. B.; Webb, G.; Cullis, P. R. *Biochim. Biophys. Acta* **1985**, *812*(1), 55–65.

(17) Alig, A. R. G.; Gourdon, D.; Israelachvili, J. J. *Phys. Chem. B* **2007**, *111*(1), 95–106.

(18) Israelachvili, J. N.; Adams, G. E. *J. Chem. Soc., Faraday Trans. I* **1978**, *74*, 975–1001.

(19) Vigil, G.; Xu, Z. H.; Steinberg, S.; Israelachvili, J. J. *Colloid Interface Sci.* **1994**, *165*(2), 367–385.

(20) Walker, S. L.; Bhattacharjee, S.; Hoek, E. M. V.; Elimelech, M. *Langmuir* **2002**, *18*(6), 2193–2198.

(21) Scales, P. J.; Grieser, F.; Healy, T. W.; White, L. R.; Chan, D. Y. C. *Langmuir* **1992**, *8*(3), 965–974.

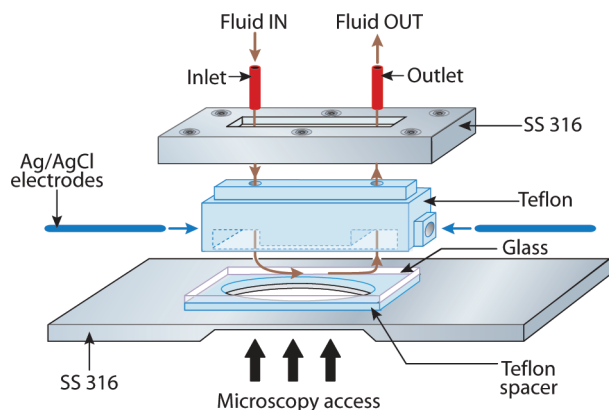


Figure 1. Schematic of the streaming potential apparatus.

streaming potential measurements, E , were done at five or more different pressures P to obtain the slope $\Delta E/\Delta P$. The slope was converted to the zeta-potential ζ using the modified Helmholtz–Smoluchowski (H-S) equation:²⁰

$$\frac{E}{P} = \frac{\epsilon_0 \epsilon_r}{\eta \lambda} \frac{(\zeta_{\text{Teflon}} + \zeta_{\text{glass}})}{2} = \frac{\epsilon_0 \epsilon_r \zeta_{\text{average}}}{\eta \lambda} \quad (1)$$

where ϵ_0 and ϵ_r are the permittivity of free space and the relative permittivity of the electrolyte solution, respectively, η is the viscosity of the electrolyte solution, and λ is its conductivity. Zeta potentials were measured as a function of total lipid approximately 10 min after the solution was introduced into the cell. Nonmetallic injectors were used to avoid the possibility of multivalent ions, for example, Fe^{3+} , adsorbing to any of the negatively charged surfaces.

Theoretical Analysis of Neutral Bilayer-Charged Substrate Interactions

Interactions between neutral (uncharged, zwitterionic) bilayers and solid substrates (e.g., glass) include the van der Waals, double-layer, hydration, hydrophobic, thermal undulation, and protrusion forces. These forces are very different between bilayers in solution versus bilayers interacting with a solid, rigid, and chemically different substrate surface (glass in our studies).

For a bilayer (medium 1) of thickness T whose surface is at a distance D away from a silica surface (medium 3) in an aqueous medium (medium 2), the nonretarded van der Waals force between them is approximated by the expression:²²

$$F_{\text{VDW}}(D) = -\frac{A_{123}}{6\pi} \left(\frac{1}{D^3} - \frac{2}{(D+T)^3} + \frac{1}{(D+2T)^3} \right) \quad (2)$$

where the Hamaker constant A_{123} is typically $(3-4) \times 10^{-21}$ J in concentrated salt solutions. For “symmetrical” systems, this force is always attractive, but between dissimilar surfaces, as in our experiment, it can be either attractive or repulsive. Note that at small separations, when $D \ll T$, the force (per unit area) asymptotes to

$$F_{\text{VDW}}(D) = -\frac{A_{123}}{6\pi D^3} \text{ N m}^{-2} \text{ (Pa)} \quad (3)$$

and the energy (per unit area) asymptotes to

$$W_{\text{VDW}}(D) = -\frac{A_{123}}{12\pi D^2} \text{ N m}^{-1} \text{ (J m}^{-2}) \quad (4)$$

The double-layer interaction for this *asymmetric* system of an uncharged bilayer and a charged (silica) surface is complex. An approximate equation for two planar surfaces of low, unequal but constant potentials (< 25 mV) in a 1:1 electrolyte is the “Hogg–Healy–Fuerstenau” (HHF) equation:²³

$$W_{\text{DL}}(D) = \frac{\epsilon_0 \epsilon_r \kappa \left[2\psi_1 \psi_2 - (\psi_1^2 + \psi_2^2) e^{-\kappa D} \right]}{(e^{+\kappa D} - e^{-\kappa D})} \text{ J m}^{-2} \quad (5)$$

D. Y. C. Chan (private communication) has verified that the HHF equation is an excellent approximation to the exact, non-linear solution to the PB equation, even for much higher potentials than $|25|$ mV. It thus remains applicable for silica surfaces, which have a potential of about -50 mV that can be adjusted by the ionic strength and pH.

To a first approximation, we may equate ψ with ζ since both are determined by the Poisson–Boltzmann equation; that is, they do not include the Stern layer potentials.²⁴ In the case of a PC bilayer interacting with a silica surface, since the zwitterionic surface of PC is neutral (uncharged), its potential is zero, $\psi_2 = 0$ for the bilayer surface, and $\psi_1 = \psi_0$ for the silica surface which simplifies the HHF equation to

$$W(D) = \frac{-\epsilon_0 \epsilon_r \kappa \psi_0^2 e^{-\kappa D}}{(e^{+\kappa D} - e^{-\kappa D})} \quad (6)$$

Thus, the double layer interaction is *attractive* at all separations. (Note: for $\psi_2 \neq 0$, the large distance limit can be either attractive or repulsive; for example, for similar but unequal potentials, the double layer force changes sign at some separation close to the Debye length from attractive at small separations to repulsive at large separations). Figure 2 shows representative theoretical plots of the double layer and van der Waals interactions. In the limit of large and small distances, eq 6 gives

$$\text{at large separations } (\kappa D \gg 1) : W(D) \rightarrow -\epsilon_0 \epsilon_r \kappa \psi_0^2 e^{-2\kappa D} \quad (7)$$

$$\text{at small separations } (\kappa D \ll 1) : W(D) \rightarrow -\epsilon_0 \epsilon_r \psi_0^2 e^{-\kappa D} / 2D \quad (8)$$

Thus, the attraction increases with the magnitude of ψ_0 irrespective of the sign of the potential. Putting $\psi_0 = -(50-75)$ mV for the silica surface and $D = D_0 = 0.5$ nm for the contact (cutoff) separation, we obtain $W(D_0) \approx -(1-2)$ mJ m⁻² for the double-layer contribution to the adhesion energy. This is a large value, much larger than any of the other calculated forces.

It is important to contrast these predictions for interactions between surfaces of constant potential with those that result between surfaces of constant charge. Approximate expressions for constant charge interactions between dissimilar surfaces are more complicated. The following, proposed by Gregory, is

(23) Hogg, R.; Healy, T. W.; Fuerstenau, D. W. *Trans. Faraday Soc.* **1966**, *62*, 1638–1651.

(24) Hunter, R. J.; Ottewill, R. H. *Zeta potential in colloid science: principles and applications*; Academic Press: London, 1981.

(22) Israelachvili, J. N. *Intermolecular and Surface Forces*, 2nd ed.; Academic Press: London, 1992.

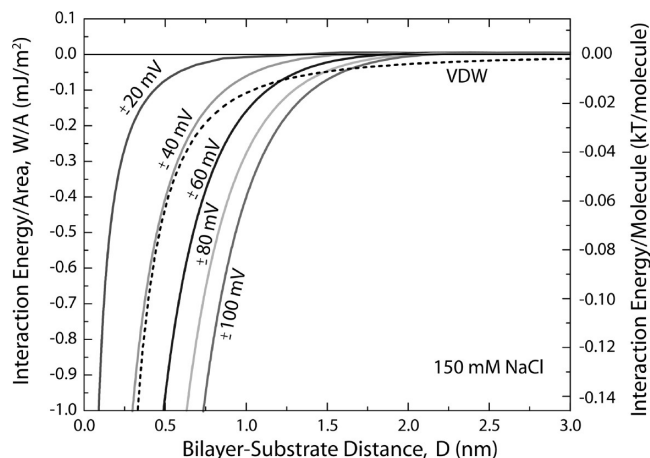


Figure 2. Theoretical surface energy curves from the HHF equation for a planar uncharged bilayer ($\psi_0 = 0$ mV) against a parallel, solid silica substrate in PBS. Assumes constant potential surfaces. The VDW interaction is shown for comparison.

probably the simplest that is also reasonably accurate for 1:1 electrolytes:²⁵

$$P(D) = \rho_{\infty} kT \left[2 \left\{ 1 + \left(\frac{ze(\psi_1 + \psi_2)/kT}{e^{+\kappa D/2} - e^{-\kappa D/2}} \right)^2 \right\}^{1/2} - \frac{\{ze(\psi_1 - \psi_2)/kT\}^2 e^{-\kappa D}}{1 + \left(\frac{ze(\psi_1 + \psi_2)/kT}{e^{+\kappa D/2} - e^{-\kappa D/2}} \right)^2} - 2 \right] \text{ N m}^{-2} \quad (9)$$

Notice that, for dissimilar surfaces with $\psi_1 = 0$ and $\psi_2 = \psi_0$, the constant charge interaction is repulsive at all separations, similar to that between two symmetrical surfaces. Constant charge interactions are always repulsive at small separations ($D \rightarrow 0$) for any potentials due to the osmotic pressure of the trapped counterions: $P(\kappa D \rightarrow 0) = +|(\psi_1 + \psi_2)kT/zeD|$. Therefore, we see that the nature of the interaction between a bilayer and charged surface depends on the nature of the surfaces, that is, whether constant charge or constant potential or somewhere in between (“charge regulation”).²⁶

Results and Discussion

Surface Potential Measurements of Adsorbing DMPC Bilayers. Figure 3 shows the drop in the magnitude of the ζ potential with increasing DMPC exposure in the cell, indicative of increasing coverage of the borosilicate surface, presumably by neutral (uncharged) DMPC bilayers. Such a trend is consistent with an attractive electrostatic force between the neutral DMPC bilayer and the charged (borosilicate) surface assuming a constant potential interaction as represented by the HHF equation, eq 6. The measured potential is that of the double layer at the bilayer-on-glass surface and represents the residual or incomplete neutralization of the glass–bilayer interface. The magnitude of the potential decreases sharply when $N \approx 20$, implying that a “threshold density” of vesicles is required to trigger vesicle rupture and the beginning of bilayer formation on the surface (details to be published elsewhere²⁷).

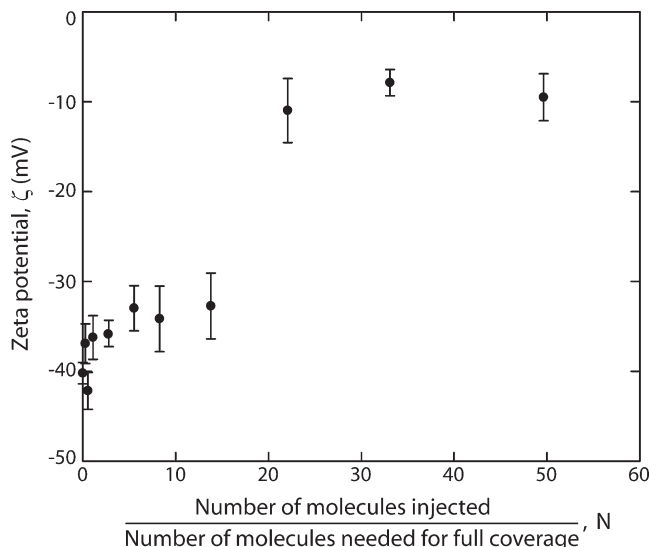


Figure 3. Zeta potential, ζ , of borosilicate glass as a function of the normalized amount of DMPC injected into the cell, defined as $N = \text{amount injected/amount for full surface coverage}$, where full surface coverage was calculated assuming a surface area of 47 \AA^2 per lipid per monolayer in the bilayer at $20 \text{ }^\circ\text{C}$.²⁸ The cell contained a 100 mM KCl solution.

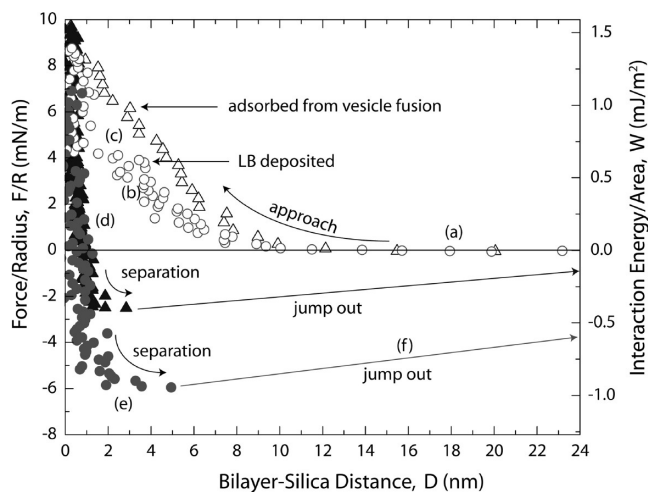


Figure 4. Force–distance profiles for two representative force runs between a silica surface and a DMPC bilayer prepared on mica by vesicle fusion (black triangles) and LB deposition (gray circles) in 150 mM NaCl PBS solution at $28 \text{ }^\circ\text{C}$ (fluid state bilayers) under conditions where the DMPC–mica surface potential was small. In both cases, the surfaces were brought together (open points) into bilayer–silica contact at $D = 0$ and then separated (closed points). The letters (a)–(f) label the different stages of the force runs illustrated in Figure 5.

Surface Force Measurements. Figure 4 shows the force–distance profiles measured between a silica surface and two types of (differently prepared) DMPC bilayers adsorbed on mica in PBS solution. The results show quantitative differences between bilayers prepared by vesicle fusion and LB deposition. For both types of bilayer, there is a repulsive interaction at distances ≤ 10 nm, however, in the case of bilayers formed by vesicle fusion, the repulsion upon approach is stronger, possibly due to a combination of higher undulation forces of these presumably more loosely adsorbed bilayers and larger double-layer forces

(25) Gregory, J. J. *Colloid Interface Sci.* **1975**, *51*(1), 44–51.

(26) Ben-Yaakov, D.; Burak, Y.; Andelman, D.; Safran, S. A. *EPL* **2007**, *79*(4), 48002.

(27) Min, Y.; Pesika, N.; Zasadzinski, J. A.; Israelachvili, J. N. In preparation.

(28) Marsh, D. *CRC handbook of lipid bilayers*; CRC Press: Boca Raton, FL, 1990.

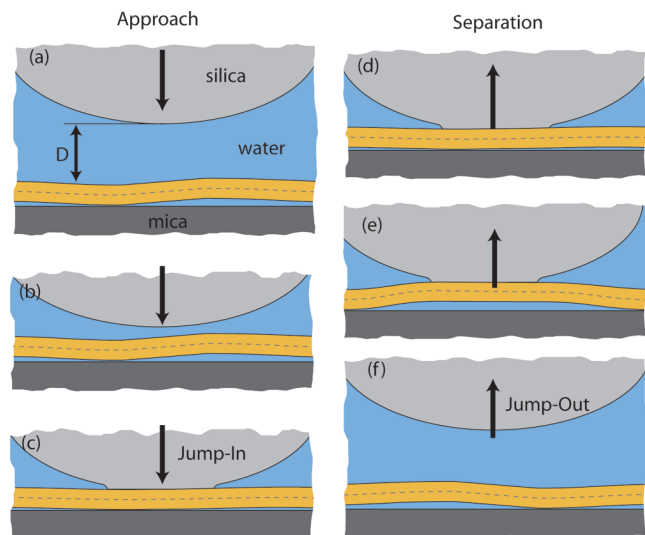


Figure 5. Schematics of surfaces in the SFA during a force run. (a) Upon approach, the surfaces are driven together at a constant velocity. (b) The silica feels an initial repulsion due to repulsive undulation and hydration forces. (c) The repulsive barrier is overcome, and the surfaces jump into adhesive contact. (d, e) The surfaces are pulled apart but stay in adhesive contact as the force measuring spring is decompressed. (f) The spring force equals the adhesion force and the surfaces jump apart. The forces at the six panels labeled (a)–(f) are indicated by the same letters in Figure 4.

due to the residual double-layer potential (see Figure 3, also discussed further below). This larger repulsion results in smaller jumps in and out of adhesive contact seen in the force profiles for bilayers formed by vesicle fusion.

The bilayer–silica adhesion energies, W , corresponding to the adhesion forces, F_{ad} , for each type of bilayer, calculated using the Derjaguin approximation,²² $W = F/2\pi R$, are plotted on the right-hand ordinate of Figure 4. Our results in PBS solution show that the adhesion energies vary between 0.5 and 1.0 mJ m^{-2} , depending on the bilayer preparation; these energies are much larger than the adhesion of two (symmetrical) PC bilayers ($\sim 0.1 \text{ mJ m}^{-2}$)^{2,29} or the adhesion predicted by the VDW interaction between DMPC and silica using eq 1 ($\sim 0.1 \text{ mJ m}^{-2}$) but close to the values of 1–2 mJ m^{-2} predicted by the HHF equation (eq 7 and Figure 2), suggesting that the high adhesion energies are due to an electrostatic attraction between the uncharged bilayer and silica surface.

A strong electrostatic attraction between these asymmetric surfaces appears to be why uncharged PC vesicles readily adhere, deform, rupture, and spread as bilayers on silica but do not adhere (or only very weakly)^{2,29} or fuse to each other in solution, or why silica surfaces do not adhere to each other in aqueous solutions.

The stronger adhesion measured between LB-deposited bilayers compared to those adsorbed from vesicles (Figure 4) is likely to be due to the higher tensile stress (tension) of LB bilayers, which suppresses their undulations and therefore the repulsive thermal undulation force. Also, the potentials of LB-deposited surfaces (mica or silica) are generally uncharged and exhibit no double-layer repulsion²⁹ because the first (hydrophobic) layer deposited neutralizes the surface on exposure to air, whereas the same surface retains some of its charge (potential) when the lipids adsorb straight from solution.³⁰

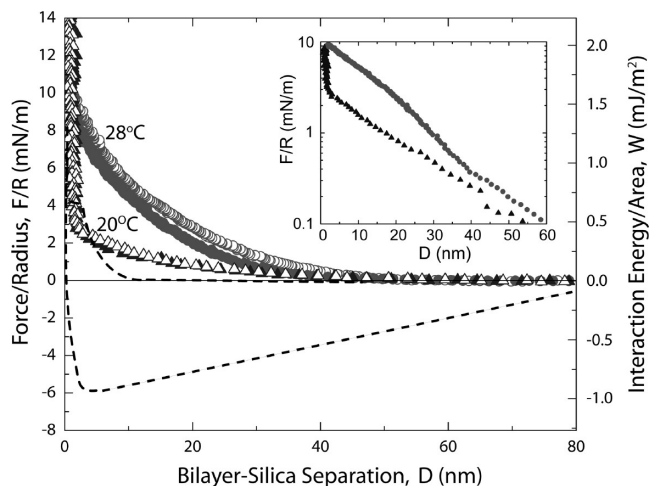


Figure 6. Force–distance profiles of LB-deposited bilayer–silica interactions in distilled water above (28 °C) and below (20 °C) the chain melting temperature of DMPC ($T_m = 24 \text{ °C}$). The curves are purely repulsive and show little hysteresis between approach (open symbols) and separation (closed symbols). The inset shows the same data plotted on a log scale. Dashed lines: LB-deposited bilayers at 28 °C in PBS (taken from Figure 4).

The -10 mV residual potential measured in the streaming potential experiments (Figure 3) is a manifestation of this effect, which could also contribute to the differences observed in the forces.

The major driving force for adhesion (adsorption/spreading) is therefore the electrostatic attraction between the uncharged PC bilayer and the charged silica surface. According to eq 6, this force should increase with the zeta potential, ζ , or charge density, σ , of the (silica or glass) surface, but be indifferent to whether the charge is positive or negative. This is consistent with the previous experiments by Cha et al.,³¹ who found that egg-PC vesicles do not adsorb to surfaces of low σ but do adsorb to surfaces with high σ , either negative or positive.

Further insights into bilayer–silica interactions come from studying the effects of temperature and ionic strength. Figure 6 shows force–distance profiles for the same system as in Figure 4 but in distilled water and at two different temperatures. The dashed lines show the data of Figure 4 in PBS at the higher temperature (28 °C) for comparison. Regarding the effect of temperature, the additional repulsion observed at $T > T_m$ is attributed to the increase in the repulsive fluctuation force between the now highly fluid bilayer and the glass surface.³²

The exponentially repulsive forces in Figure 6 suggest a purely electrostatic double-layer repulsion in pure water (large Debye length) between a surface of high potential, ψ_0 , interacting at constant charge (cf. theory section). It is known that the magnitude of the (negative) surface potential of silica in the pH regime studied ($\text{pH} = 7.5$) increases as the ionic strength decreases, reaching -120 mV in 10^{-4} M NaCl .²¹ Similar trends occur for borosilicate glass, another glass we studied (see below), where the potential reaches -170 mV in 10^{-4} M KCl at $\text{pH} 7.1$.³³ It is not obvious why the surfaces should interact at constant potential in high salt conditions and at constant charge in low (or no) salt. Most likely, “charge regulation”, which

(31) Cha, T.; Guo, A.; Zhu, X. Y. *Biophys. J.* **2006**, *90*(4), 1270–1274.

(32) Benz, M.; Gutsmann, T.; Chen, N. H.; Tadmor, R.; Israelachvili, J. *Biophys. J.* **2004**, *86*(2), 870–879.

(33) Van Wagenen, R. A.; Andrade, J. D.; Hibbs, J. B. *J. Electrochem. Soc.* **1976**, *123*(10), 1438–1444.

(29) Marra, J.; Israelachvili, J. N. *Biochemistry* **1985**, *24*(17), 4608–4618.

(30) Chen, Y. L.; Chen, S.; Frank, C.; Israelachvili, J. J. *Colloid Interface Sci.* **1992**, *153*(1), 244–265.

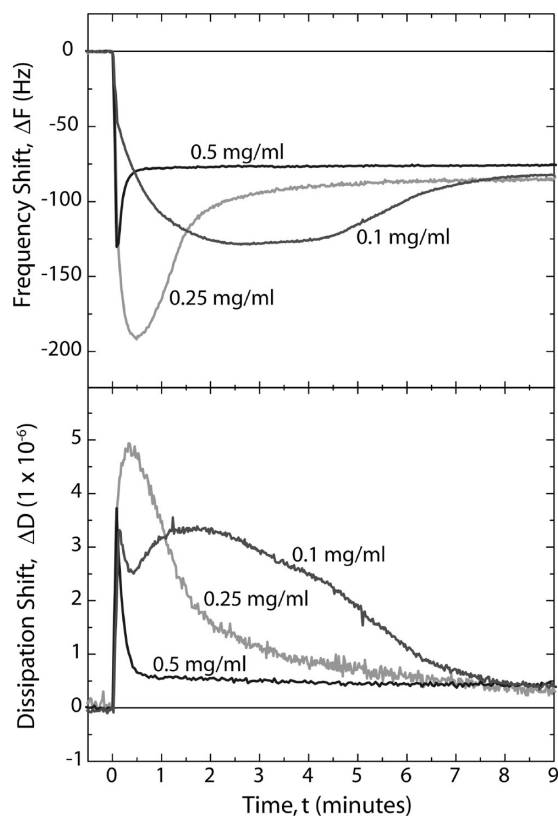


Figure 7. QCM results showing the effect of DMPC concentration on the adsorption of vesicles to silica surfaces in PBS (pH 7.4) at $T = 28\text{ }^{\circ}\text{C}$. The vesicles adsorb and rupture, leaving a single bilayer on the surface, consistent with the strong adhesion evidenced by SFA experiments.

involves the exchange of surface ions with the bulk reservoir as the surfaces approach each other is occurring, which is reduced in lower salt when there are fewer ions in the bulk solution. (The above is an equilibrium explanation. In dilute solutions, kinetics or rate effects have also been observed to suppress charge regulation.³⁴) Thus, in dilute solution, the silica interacts at constant charge and thus gives an electrostatic *repulsion* described by eq 9, while in concentrated solution the interaction is at constant potential, giving rise to an *attraction* as described by eq 6.

Vesicle Fusion Studied by QCM and FRAP. Figure 7 shows an effect of vesicle concentration on bilayer formation in PBS solution. The initial adsorption of the vesicles to the silica is observed as a decrease in the resonant frequency of the quartz crystal and an increase in the dissipation measurement. As the vesicles rupture and release their water, the frequency and dissipation recover until they reach a constant value. The final frequency shift of $\sim 75\text{--}80\text{ Hz}$ shown in Figure 7 corresponds to an adsorbed mass of $\sim 442\text{--}472\text{ ng cm}^{-2}$ according to the Sauerbrey equation using a 5 MHz QCM crystal measured at the third harmonic. An adsorbed DMPC bilayer with a head-group area³⁵ of 59 \AA^2 will have a mass of 384 ng cm^{-2} . The difference may be attributed to a trapped water layer (hydration layer between the silica and bilayer) of $\sim 0.6\text{--}0.9\text{ nm}$ thick. The measurements are thus in good agreement with the formation of a complete bilayer. Additionally, the final dissipation shift is very small ($\sim 5 \times 10^{-7}$), indicating a flat structure on

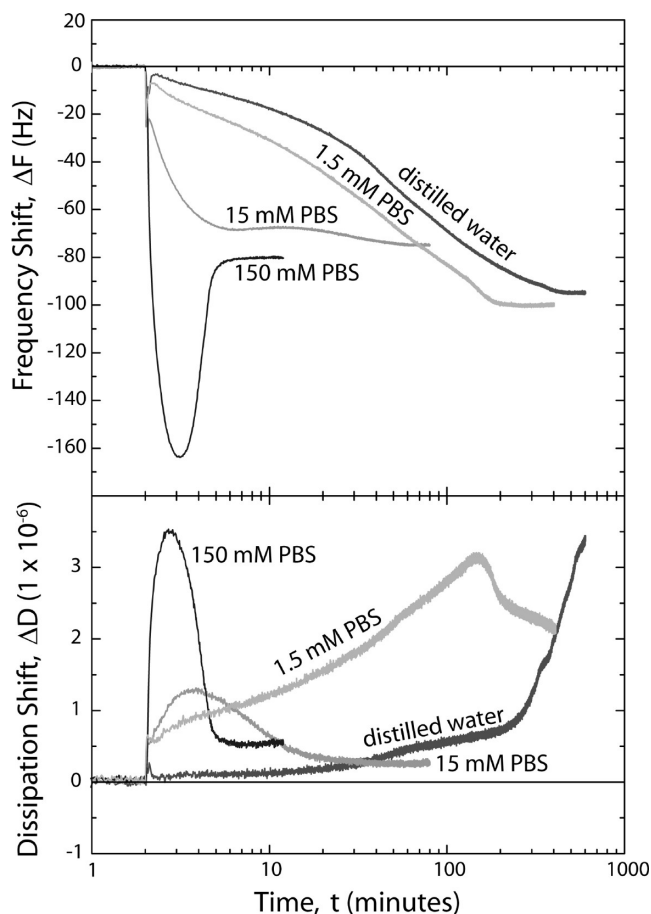


Figure 8. QCM results showing the effect of ionic strength on the adsorption of 0.1 mg/mL solution of DMPC vesicles to silica surfaces at $T = 28\text{ }^{\circ}\text{C}$. A bilayer forms in 150 mM PBS and 15 mM PBS but not in 1.5 mM PBS and distilled water. The adsorbed mass in 1.5 mM PBS and distilled water is likely due to adsorbed vesicles that do not rupture to form bilayers, consistent with the persistence of high dissipation. Also note that the rate of adsorption of mass slows as the salt concentration is reduced.

the surface, also consistent with a planar bilayer. Weirich et al.³⁶ have observed that a small fraction ($\sim 5\%$) of the lipids on the surfaces are probably vesicles weakly adsorbed to the surface bilayer. Increasing the concentration of vesicles in the solution results in faster bilayer formation, in agreement with previous results.^{14,37}

The effect of salt concentration on the adsorption and rupture of vesicles was also studied with the QCM technique (Figure 8). Here, 0.1 mg/mL vesicle solutions were prepared in PBS solutions of 150 , 15 , and 1.5 mM monovalent salt and in distilled water. No osmotic stress was induced across the bilayers of the vesicles after their formation. It appears that in 150 mM and, to a lesser extent, in 15 mM PBS, vesicles readily adsorb and rupture to form bilayers. However, in 1.5 mM PBS and distilled water, vesicles adsorb very slowly, as shown by a decrease in the QCM resonant frequency, but do not rupture to form bilayers—but rather form soft or “floppy” structures on the surfaces, as indicated by the high dissipation. The rate of adsorption of mass to the silica surface decreases as the salt concentration is reduced regardless of the final form of the structure on the surface. There appears to be a critical salt concentration between

(34) Raviv, U.; Laurat, P.; Klein, J. *J. Chem. Phys.* **2002**, *116*(12), 5167–5172.

(35) Koenig, B. W.; Strey, H. H.; Gawrisch, K. *Biophys. J.* **1997**, *73*(4), 1954–1966.

(36) Weirich, K. L.; Israelachvili, J.; Fygenson, D. K. In preparation.

(37) Keller, C. A.; Glasmaster, K.; Zhdanov, V. P.; Kasemo, B. *Phys. Rev. Lett.* **2000**, *84*(23), 5443–5446.

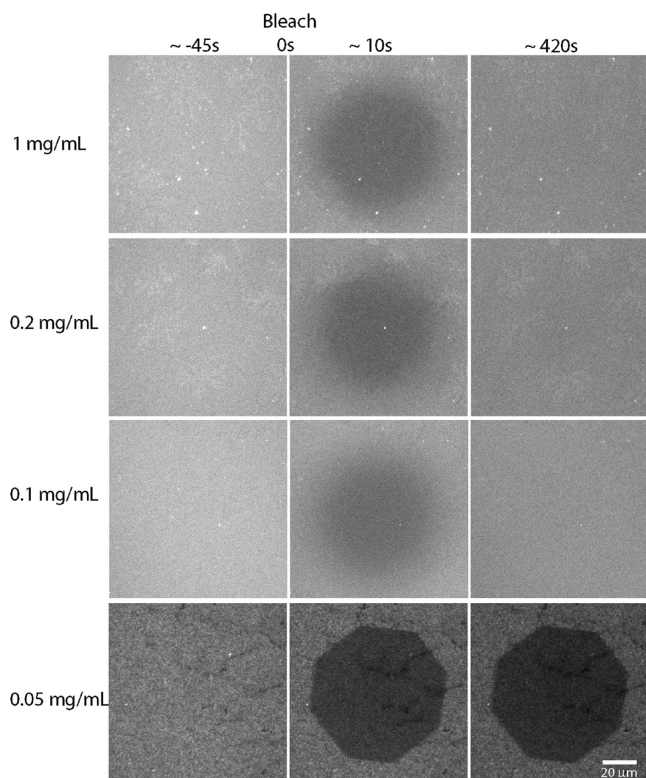


Figure 9. Fluorescence recovery of a photobleached spot on silica surfaces exposed to a maximum of $50 \mu\text{L}$ of lipid solution at four different concentrations (for ≤ 5 min). When recovery is observed, the spot recovers quickly ($\tau \sim 142 \pm 22$ s), indicating a continuous bilayer. At or below 0.05 mg/mL lipid concentration, the spot does not recover, indicating that continuous bilayers do not form, probably due to insufficient amount of lipid to fully cover the surface (see text).

15 and 1.5 mM PBS at which vesicles no longer rupture to form bilayers on the silica surface.

Taken with our SFA results in 150 mM PBS and distilled water, it appears that the adhesion between the vesicles and silica decreases as the salt concentration is reduced. It should be noted that some mass does adsorb to the silica surface even in distilled water in the QCM experiments, while our SFA measurements show purely repulsive forces between bilayer and silica in these conditions. This apparent discrepancy is attributed to a van der Waals minimum that theory shows still exists between the vesicle and silica in distilled water (regardless of the sign or magnitude of the electrostatic interaction) but is too weak to measure with the SFA. The weak minimum may be significant enough to couple a few vesicles to the silica surface even if it is not strong enough to hold them tightly. It is certainly not capable of causing them to rupture and form bilayers. Note that an adsorbed vesicle will appear as a large mass in the QCM experiment due to the water trapped inside it. A few adsorbed vesicles in distilled water can cause a frequency shift greater than an adsorbed bilayer in 150 mM PBS in Figure 8.

The process of vesicles transforming from isolated adhering vesicles to complete single bilayers on glass surfaces was further investigated by fluorescence microscopy (FM) and FRAP experiments. Figures 9 and 10 show FRAP experiments at various stages of bilayer formation, while Figure 11 shows the stability of the formed bilayers to changes in the temperature or solution conditions (i.e., to the robustness of the deposited bilayers).

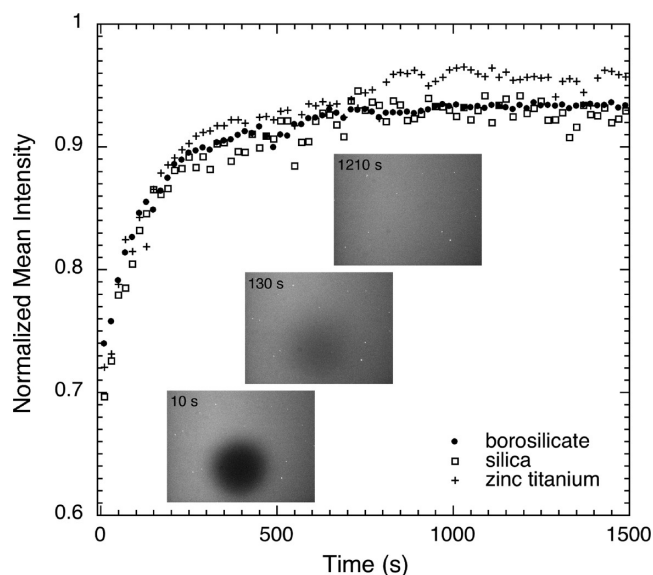


Figure 10. FRAP showing qualitatively similar recovery on silica, borosilicate, and zinc-titanate (ZnTi) glass surfaces, all tested under the same solution conditions. Images ($166 \times 225 \mu\text{m}$) shown are representative of the raw data. Intensity averaged over a region ($r = 20 \mu\text{m}$) centered around the bleached spot is plotted versus time for each of the surfaces.

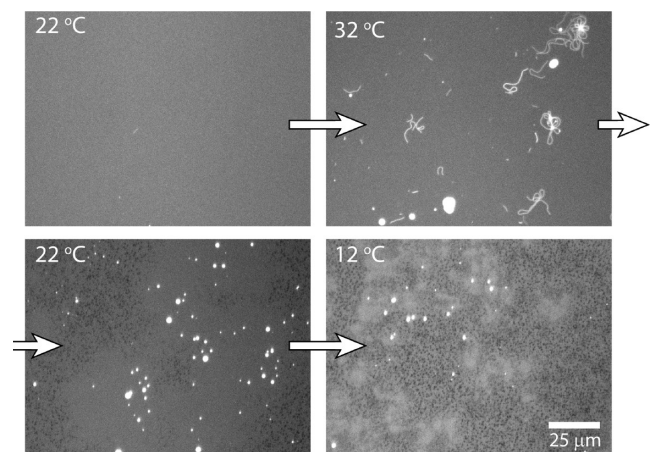


Figure 11. Fluorescence microscope images of DMPC bilayers on borosilicate glass soon after formation ($22 \text{ }^\circ\text{C}$), after raising the temperature ($32 \text{ }^\circ\text{C}$), lowering it again ($22 \text{ }^\circ\text{C}$) and cooling ($12 \text{ }^\circ\text{C}$). Upon raising the temperature, bright linear structures (worms) grow out of the bilayer and some collapse into bright round structures. Upon cooling, all linear structures collapse and some dark holes appear, suggesting that lipid from the surface was lost into the collapsed structures. Further cooling to below T_p has no discernible effect.

Figure 9 shows lipid coverage of surfaces exposed to different amounts of lipid in solution at room temperature ($\sim 22 \text{ }^\circ\text{C}$). At all but the lowest concentration shown, the coverage is a uniform and continuous bilayer, as indicated by the rapid FRAP ($\tau \sim 142 \pm 22$ s (s.d. for $n = 7$)). At 0.05 mg/mL DMPC and lower, the coverage is inhomogeneous and no recovery is observed.

These results reinforce the notion that the formation of a continuous bilayer requires the surface to be exposed to a minimal amount of lipid. Given the geometry of our flowcell, which presents $\sim 308 \text{ mm}^2$ of glass substrate to the solution, and an area per headgroup²⁸ of 0.47 nm^2 , approximately 1.3×10^{15} lipid molecules are needed to cover the glass with a complete

bilayer. In the 50 μL volume of 0.05 mg/mL solution that was rinsed through the flowcell ($\sim 15 \mu\text{L}$ capacity), there was potentially 1.7 times more lipid molecules than necessary to form a complete bilayer. However, the majority of the 50 μL was passed through the flowcell in only a few seconds (so as to thoroughly replace the lipid-free buffer solution), and the surface was incubated with only the final $\sim 15 \mu\text{L}$ solution (for 5 min before rinsing). Assuming no lipid deposited while exchanging solution, the surface was exposed to only half as much lipid as needed for a complete bilayer at this lowest lipid concentration. At twice that concentration (0.1 mg/mL), a continuous bilayer did form, suggesting that the very minimum amount of lipid in the bulk needed to form a complete bilayer may well suffice to do so.

Continuous bilayers formed by exposing the silica substrates to different amounts of lipid vesicles have indistinguishable recovery times. This suggests that the bilayer formed does not depend on the excess amount of available lipid. Continuous bilayers adsorbed on different types of glass also have similar recovery times (Figure 10). The recovery times at 28 $^{\circ}\text{C}$ are ~ 144 , 161, and 179 s for silica, borosilicate, and zinc titanium, respectively. This suggests that all three of these types of glass interact similarly with the bilayers.

Once formed, the adsorbed bilayers are “robust” but only if certain conditions are met. Essentially, these require that the solution conditions do not change, with certain properties being more important than others. The most important appears to be the temperature, especially when the temperature of the system is close to the chain melting temperature of the surfactant ($T_m = 24 \text{ }^{\circ}\text{C}^{38}$ in the case of DMPC). Figure 11 shows that increasing the temperature then decreasing it again can lead to irreversible changes, indicating the fragility of the adsorbed bilayers to temperature changes, especially when the changes involve passing through the chain melting temperature, T_m , and pretransition temperature, T_p , which is a few degrees below T_m but not as sharply defined. The storage conditions must therefore be carefully monitored to ensure the long-term stability and robustness of these supported bilayers.

Conclusions

The Mechanism of Spreading. Our findings suggest that a number of distinct stages occur during the adsorption of a bilayer on a charged surface such as glass. Under sufficiently adhesive conditions, vesicles can adsorb to the substrate surface. If the adhesion is strong enough or the vesicle is in a stressed state (e.g., osmotically),¹⁴ the vesicle may deform and cause interbilayer stresses sufficient enough to cause the vesicle to rupture, forming a bilayer island on the surface.¹¹ If the strength of adhesion is not strong enough to rupture isolated vesicles on the surface (as is the case with PC bilayers on silica), the vesicles require additional stresses from neighboring vesicles to cause rupture, that is, a critical vesicle concentration on the silica.³⁹ After initial rupture of vesicles, subsequent vesicles can fuse with the unfavorable edges of the bilayer patches through hydrophobic interactions between the tails of the lipids in the highly curved regions of the bilayer edge and stressed vesicle. This process continues until the bilayer is complete, at which point excess lipid and water may be ejected back into solution.⁴⁰

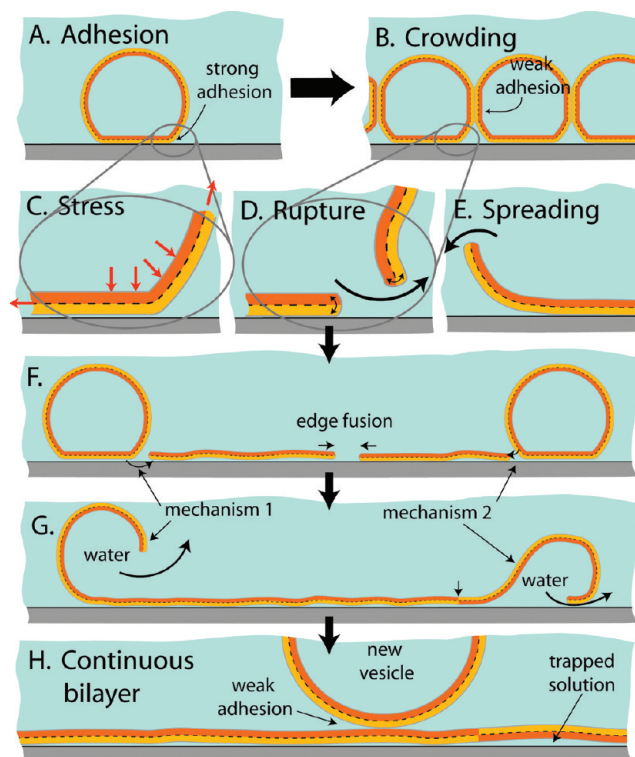


Figure 12. Different stages of vesicle adsorption: (A) adhesion, (B) crowding, (C–E) stress-induced rupture and spreading of bilayer patches that can expose either leaflet by either mechanism 1 or 2, (F, G) coalescence of high energy edges and expulsion of water and excess lipid, and (H) growth of patches into a continuous bilayer; further adsorption of vesicles to the bilayer is weak and does not lead to their rupture or spreading.

Note that vesicles can rupture to expose either the inner or outer leaflet of their membrane. Our experiments do not allow us to distinguish between these two mechanisms. The different stages are illustrated in Figure 12.

Optimizing Vesicle Fusion. For the case of the adsorption of neutral lipids onto charged substrate surfaces, as studied here, we find that a number of conditions need to be satisfied for attaining homogeneous single bilayers:

- (1) high vesicle concentration ($> 0.1 \text{ mg/mL}$);
- (2) medium to high substrate surface potential;
- (3) high ionic strength;
- (4) temperature above the chain melting temperature.

Depending on the vesicle size and concentration, and the surface and solution conditions, some of the stages are reversible, for example, $A \leftrightarrow B$, while others are not, for example, $F \rightarrow G$. Once bilayers are formed, they are robust; however, on diluting the solution or increasing the temperature, some or all of the bilayer will eventually come off,^{29,41} but this process goes through different stages than the reverse of those shown in Figure 12, for example, through the outgrowth of tubular vesicles that pinch off from the supported bilayer. Temperature changes appear to act quickly, while changing the vesicle concentration causes much slower changes.

We conclude that the electrostatic double-layer interaction is the most important leading to the strong attraction and adhesion of neutral or weakly charged bilayers to charged hydrophilic surfaces. The only other attractive force, the van der

(38) Kapitza, H. G.; Ruppel, D. A.; Galla, H. J.; Sackmann, E. *Biophys. J.* **1984**, *45*(3), 577–587.

(39) Reimhult, E.; Hook, F.; Kasemo, B. *J. Chem. Phys.* **2002**, *117*(16), 7401–7404.

(40) Stroumpoulis, D.; Parra, A.; Tirrell, M. *AIChE J.* **2006**, *52*(8), 2931–2937.

(41) Helm, C. A.; Israelachvili, J. N. *Makromol. Chem., Macromol. Symp.* **1991**, *46*, 433–437.

Waals forces, is relatively weak and incapable of inducing sufficient stresses to cause rupture, which is a prerequisite for spreading. It is not possible to provide a general equation for the interaction potential between a neutral bilayer and a charged surface that is valid under all conditions because the system may be a “charge regulating” one, namely, interacting neither at constant surface potential nor at constant charge. Most systems

fall in between these two limits. Maximum adhesion is expected for systems that interact at constant potential.

Acknowledgment. We would like to thank Derek Y. C. Chan for his advice on electrostatic double-layer interactions and Emily Meyer for lending her expertise on bilayers and SFA measurements. This work was funded by Corning Incorporated.